Spatial Mapping and Size Distribution of Oxidative Potential of Particulate Matter Released by Spatially Disaggregated Sources

Lorenzo Massimi[1,*], Martina Ristorini[2], Giulia Simonetti[1], Maria Agostina Frezzini[1], Maria Luisa Astolfi[1], Silvia Canepari[1]

[1] Department of Chemistry, Sapienza University of Rome, P. le Aldo Moro, 5, Rome 00185, Italy;

[2] Department of Bioscience and Territory, University of Molise, Pesche (IS), 86090, Italy.

[*]Correspondence: **l.massimi@uniroma1.it**

Keywords: Spatial variability; Size distribution; PM source; Ascorbic acid (OP^{AA}) assay; 1,4-dithiothreitol (OP^{DTT}) assay; 2',7'-dichlorodihydrofluorescein (OP^{DCFH}) assay

Abstract: The ability of particulate matter (PM) to induce oxidative stress is frequently estimated by acellular oxidative potential (OP) assays, such as ascorbic acid (AA) and 1,4-dithiothreitol (DTT), used as proxy of reactive oxygen species (ROS) generation in biological systems, and particle-bound ROS measurement, such as 2',7'-dichlorodihydrofluorescein (DCFH) assay. In this study, we evaluated the spatial and size distribution of OP results obtained by three OP assays (OP^{AA}, OP^{DCFH} and OP^{DTT}), to qualitative identify the relative relevance of single source contributions in building up OP values and to map the PM potential to induce oxidative stress in living organisms. To this aim, AA, DCFH and DTT assays were applied to size-segregated PM samples, collected by low-pressure cascade impactors, and to PM_{10} samples collected at 23 different sampling sites (about 1 km between each other) in Terni, an urban and industrial hot-spot of Central Italy, by using recently developed high spatial resolution samplers of PM, which worked in parallel during three monitoring periods (February, April and December 2017). The sampling sites were chosen for representing the main spatially disaggregated sources of PM (vehicular traffic, rail network, domestic heating, power plant for waste treatment, steel plant) present in the study area. The obtained results clearly showed a very different sensitivity of the three assays toward each local PM source. OP^{AA} was particularly sensitive toward coarse particles released from the railway, OP^{DCFH} was sensible to fine particles released from the steel plant and domestic biomass heating, and OP^{DTT} was quite selectively sensitive toward the fine fraction of PM released by industrial and biomass burning sources.

1. Introduction

Particulate matter (PM) air pollution is one of the major risk factors for human health worldwide (Anderson et al., 2012; Lubczyńska et al., 2017). Various epidemiological studies have spotlighted strong correlations between exposure to PM and the onset of cardiovascular and respiratory diseases (Pope and Dockery, 2006). Indeed, over the years, it has been associated to a great number of adverse outcomes for human health, such as respiratory and cardiovascular diseases, cancer, diabetes, metabolic disorders, atherosclerosis and neurodegenerative diseases (Strak et al., 2012; Gupta et al., 2019; Øvrevik et al., 2019). Several epidemiological studies have spotlighted strong correlations between PM exposure and the onset of cardiopulmonary diseases (Brunekreef et al, 2002; Pope et al, 2006). However, most of the studies use PM mass concentration as exposure indicator, which misestimates the overall impact of PM, since it does not take into account the multiple toxicological effects of the different pollutants that make up particulate matter. This limitation can be overcome by identifying possible relationships between PM toxicity and its specific physic-chemical properties. In fact, during the last few decades, the complex and variable composition of PM has been widely investigated and many studies have revealed that several PM properties, such as chemical composition and particle dimension, influence its health and environmental effects (Ricci and Cirillo, 1985; Hlavay et al., 2001; Kelly et al., 2012). Nevertheless, not enough evidence that associates each property to specific outcomes has been yet identified (WHO, 2013).

Nowadays, there is a growing scientific consensus in affirming that generation of reactive oxygen species (ROS) is one of the major mechanisms by which PM exerts its adverse biological effects (Li et al., 2015), leading to oxidative stress responses and thus to different chronic and acute systemic inflammations (Li et al., 2003; Esposito et al., 2014; Pirrino et al., 2017). Indeed, PM ability to generate oxidative stress in biological systems has been demonstrated to contribute to genotoxicity and cytotoxic mechanisms responsible for cell damages (Marcoccia et al., 2017; Piacentini et al., 2019). PM capacity to trigger damaging oxidative reactions and inflammations is defined as oxidative potential (OP), which is a measure of PM ability to oxidise target molecules, by generating ROS in acellular environments. Over the last years, OP has been proposed as a biologically relevant metric for addressing PM exposure (Yang et al., 2016; Simonetti et al., 2018a, 2018b; Gao et al., 2020), since it appeared to be more reliable than PM mass concentration (Delfino et al., 2011; Gupta et al., 2019). However, the variability in chemical composition of PM and in the contributions of different sources, reduces the correlation with health outcomes and may thus limit the potential of OP as a global toxicological indicator.

To date, various acellular assays for the measurement of OP, such ascorbic acid (AA), 1,4-dithiothreitol (DTT) and 2',7'-dichlorodihydrofluorescein (DCFH), have been used to estimate the

toxicity of PM released by different emission sources (Bates et al., 2019). Ascorbic acid and 1,4-dithiothreitol ($HSCH_2CH(OH)CH(OH)CH_2SH$) are strong reducing agents; DTT and AA assays involve the controlled incubation of the anti-oxidant (DTT or AA) in PM aqueous extracts under controlled conditions and the measurement of its depletion over time (Cho et al., 2005; Stoeger et al., 2008; Fang et al., 2016; Campbell et al., 2019). The antioxidant loss rate represents the capacity of PM reactive species to catalyze the transfer of electrons from AA or DTT to oxygen, providing an estimation of the OP. On the other hand, 2',7'-dichlorodihydrofluorescein assay, formerly developed for the in-vitro determination of ROS in biological cells (Lebel et al., 1992; Wang and Joseph, 1999; Halliwell and Whiteman, 2004), is today one of the most used methods for particle-bound ROS measurement in PM (Venkatachari et al., 2005, 2007). It is based on the oxidation of DCFH, a non-fluorescent reagent, to DCF, a fluorescent compound, in the presence of ROS and horseradish peroxidase (HRP), a redox enzyme that primarily reacts with hydrogen peroxide and organic hydroperoxides. The measured fluorescence intensity is converted into hydrogen peroxide equivalents, which is used as an indicator of the ROS reactivity (Hung and Wang, 2001; Perrone et al., 2016). However, each of these methods has been deemed sensible toward PM coming from different emission sources and characterized by very different physic-chemical properties (Ayres et al., 2008; Simonetti et al., 2018b; Frezzini et al., 2019; Piacentini et al., 2019). Therefore, none of the OP assays can be a-priori considered as representative of ROS generation pathways in biological organisms (Fang et al., 2015).

The knowledge of the relative relevance of the single source contributions in building up OP values can be of great help for the identification of the emission sources mainly responsible for ROS generation. Source apportionment of OP results from field campaigns have been attempted in some studies, but conflicting results were found (Fang et al., 2016; Perrone et al., 2016; Chirizzi et al., 2017; Calas et al., 2018). Therefore, this study was aimed to improve the knowledge about the existing relationships between OP values and sources of PM, useful to properly address PM mitigation measures to protect citizens health. In this study, we describe an innovative experimental approach, transferable to other monitoring campaigns, for the spatial mapping of OP^{AA}, OP^{DCFH} and OP^{DTT}, which represents a powerful tool for geo-referenced assessment of PM potential to induce oxidative stress and harmful effects on human health. This innovative approach, allows to qualitatively evaluate possible associations between OP values and different sources of PM, overcoming the use of receptor models, often used to investigate the contribution of sources to measured OP with different assays (Cesari et al., 2019). To this aim, we applied the AA, DCFH and DTT assays to the aqueous extracts of PM_{10} sampled by a recently developed very-low volume device (Massimi et al., 2017, 2019; Ristorini et al., 2020), in a wide and dense monitoring network

(23 sampling sites, about 1 km between each other) across Terni (Central Italy). The study area includes various spatially disaggregated intensive local PM sources (vehicular traffic, rail network, domestic heating, power plant for waste treatment, steel plant) (Capelli et al., 2011; Guerrini, 2012; Massimi et al., 2020a, 2020b) and is characterized by peculiar meteorological conditions that reduce air pollutants transport, thus favoring their accumulation (Ferrero et al., 2012). These factors have been associated with an increase of morbidity and mortality due to the onset of cardiovascular and respiratory environment-related diseases, which made this area of national interest for environmental remediation (SENTIERI-ReNaM, 2016) and particularly suitable for the spatial mapping of the OP of PM released by different sources. To our knowledge, the comparison of the three OP assays applied to PM_{10} spatially-resolved samples has never been undertaken so far.

To obtain a more reliable identification of the sources responsible for OP, the evaluation of the spatial variability was supported by the study of the size distribution of OP, able to provide information on the relative relevance of combustive and abrasive-mechanical sources in building up OP values (Simonetti et al., 2018a; Manigrasso et al., 2020). Furthermore, size distribution analysis of OP of PM provides information on the penetration capacity of particles responsible for OP in the respiratory system, thus resulting considerably valuable for the evaluation of exposure to PM and relative health risk.

2. Materials and Methods

2.1 Study Area

The study area is the city of Terni, of 211.90 km^2 and of about 112,000 inhabitants (Sgrigna et al., 2015), located in a basin of the Region Umbria (42° 34'N; 12°39' E), in Central Italy. The peculiar geomorphology of the Terni basin, limits air mixing and air pollutants transport, especially during the frequent winter episodes of atmospheric stability (Morini et al., 2016; Curci et al., 2015; Ferrero et al., 2012).

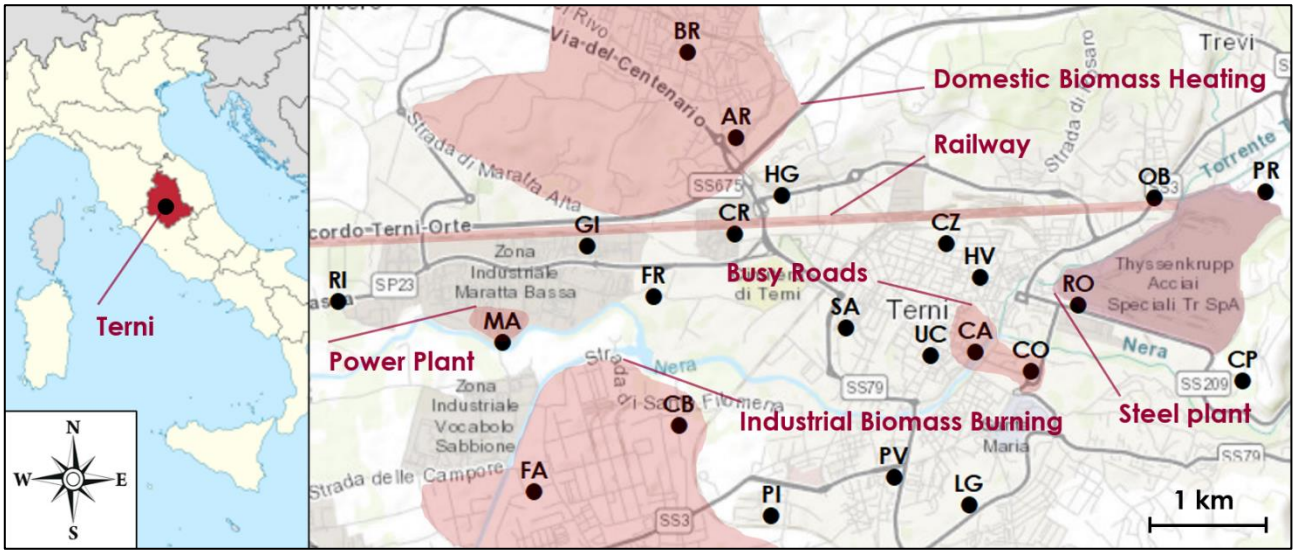

Fig. 1. Map of the 23 sampling sites in the study area (Terni, Central Italy; latitude: 42.5681, longitude: 12.6508, decimal degrees) with the location of the main local PM_{10} emission sources (ArcMap 10.3.1, ArcGis Desktop; ESRI, Redlands, CA, USA).

In Fig. 1 are shown the 23 sampling sites that were selected to cover the whole area with around 1 km spatial resolution and to study the contributions of the main local PM_{10} emission sources. In detail: RI and MA sites are located in the West of the city, near the power plant for waste treatment; GI, CR and HG are situated in the close proximity to the railway, in the North-West of the city; CZ, HV, SA, UC, CA and CO are located in the city center, between the rail network and busy roads; FA and CB, in the South-West of the city, are close to a carpentry and a craftsmanship lab and, along with PI, PV and LG, are affected by industrial biomass burning, such as the burning of carpentry waste products; FR, BR and AR, in the North of the city, are situated near townhouses frequently heated by biomass burning appliances; finally, RO, OB, PR, CP are located around the steel plant in the East of the city.

The 23 sampling sites (RI, MA, FA, GI, FR, CB, PI, BR, AR, CR, HG, SA, PV, LG, CZ, HV, UC, CA, CO, RO, OB, PR, CP) have already been studied (Massimi et al., 2017, 2019) and spatial variability of element concentrations in PM_{10} has been widely evaluated (Massimi et al., 2017, 2020a, 2020b). Spatial maps of elements tracing the main local PM_{10} sources in Terni have been obtained (Massimi et al., 2020b); therefore, localization and spatial distribution of the emission sources in the study area is well known.

2.2 Sampling Equipment

2.2.1 High Spatial Resolution Sampler

144 The High spatial resolution sampler (HSRS; FAI Instruments, Fonte Nuova, Rome, Italy) operates
145 with a very-low flow rate (0.5 L min^{-1}), it is self-powered (with a rechargeable battery and a solar
146 panel), assures long-term (1-2 months) collection of PM_{10} and has very good sampling efficiency
147 and high repeatability for stable and fine PM_{10} chemical compounds (Catrambone et al., 2019).
148 23 HSRS, equipped with 37 mm Polytetrafluoroethylene (PTFE) membrane filters (2 μm pore size,
149 PALL Corporation, Port Washington, NY, USA), were used to collect PM_{10} samples and worked in
150 parallel at the 23 sites for three monitoring periods: February (January 21st - February 20th, 2017;
151 30-day sampling), April (April 1st - May 1st, 2017; 31-day sampling) and December (November
152 25th, 2017 - January 15th, 2018; 51-day sampling) 2017, allowing the collection of 23 PM_{10} samples
153 per monitoring period.

154 *2.2.2 Micro-Orifice Uniform Deposition Impactor*
155 The Micro-orifice uniform deposition impactor (MOUDI; model 110-NR; MSP Corporation,
156 Shoreview, MN, USA) is a low-pressure cascade impactor (flow rate of 30 L min^{-1}) for the
157 collection of size-segregated PM samples through 10 impaction stages, with cut-size aerodynamic
158 diameters of 0.18, 0.32, 0.56, 1.0, 1.8, 3.2, 5.6, 10 and 18 μm.
159 Three MOUDI, equipped with 47 mm PTFE membranes (2 μm pore size, PALL Corporation, Port
160 Washington, NY, USA), were used to collect PM samples with different size fractions and worked
161 in parallel in the center (CA), West (MA) and East (PR) of the city for 20 days (February 15th -
162 March 6th, 2018).
163 Sampling efficiency and repeatability of MOUDI were assessed in Canepari et al., 2019 and in
164 Simonetti et al., 2018a. The relative repeatability for all the considered variables was found to be
165 below 10%.
166 It is worth noting that long-duration samplings carried out by MOUDI may lead to bouncing-off
167 phenomena that can be responsible for a modification of the original size distribution of
168 atmospheric particles (Canepari et al., 2019). However, to our knowledge, there are no solid and
169 recognized methods to correct the data for this artefact; furthermore, PTFE membrane filters are
170 generally considered as a suitable sampling material able to minimize the bouncing-off (Giorio et
171 al., 2013).

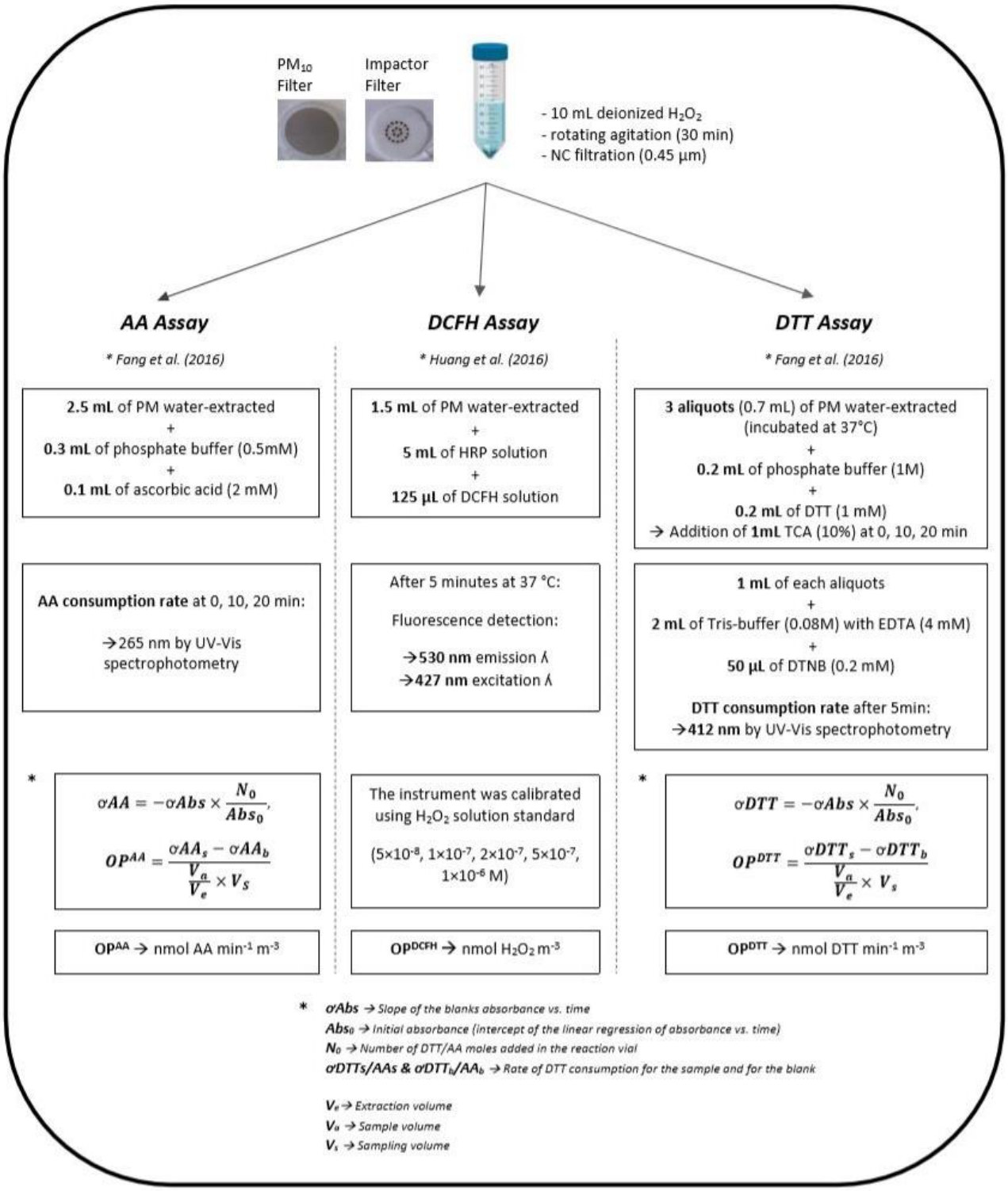

Fig. 2. Block diagram of the conducted samples preparation and OP analytical procedures for the AA, DCFH and DTT assays applied to the PM aqueous extracts.

2.3 Analytical Procedures

PTFE membrane filters were weighed before and after sampling, in order to determine PM mass concentrations. Mass concentration was determined gravimetrically by using an automated

microbalance (1 mg sensitivity, mod. ME5, Sartorius AG, Goettingen, Germany). Membrane filters were equilibrated for 2 days at 20 °C and 50% RH before and after sampling. Subsequently, PM field samples were treated by following the procedure detailed in Massimi et al. (2017, 2020a, 2020b). Briefly, after the removal of the supporting polymethylpentene ring from the PTFE membrane filter, each field filter was extracted in 10 mL of deionized water (produced by Arioso UP 900 Integrate Water Purification System, USA) by rotating agitation (60 rpm; Rotator; Glas-Col, USA) for 30 minutes, to avoid ROS generation upon ultrasonic irradiation, commonly used to efficiently extract the PM from the filters. In fact, ultrasonic waves triggers the formation and collapse of cavitation bubbles in the solution, inside which high temperatures and pressures can be reached. These conditions may lead to pyrolysis of the molecules present inside the cavitation bubbles, which results in the production of free radicals (Mutzel et al., 2013; Khurshid et al., 2014; Miljevic et al., 2014). After the extraction by rotating agitation, the obtained solution was filtered through a nitrocellulose filter (NC; pore size 0.45 µm; Merck Millipore Ltd., Billerica, MA, USA). The water-extracted solution was then split in proper aliquots for the different OP analytical procedures. Conducted samples preparation and OP analytical procedures for the AA, DCFH and DTT assays applied to the PM aqueous extracts are summarized in the block diagram of Fig. 2. Further details on the followed AA, DCFH and DTT analytical procedures and used reagents are reported in supplementary material S1. For the quality control and assurance in AA, DCFH and DTT measurements (evaluated in Simonetti et al., 2018a, 2018b and in Piacentini et al., 2019), different tests to assess the repeatability and efficiency of the three OP assays were performed in our lab on a large amount of PM field filters not stored, stored for 15 days in the fridge, in the freezer (-20°C) and at constant ambient temperature, and then extracted by ultrasonic irradiation, rotating agitation (60 rpm) and by using the vortex (2000 rpm). The obtained results showed high repeatability (10-15 %) of the OP values obtained by applying the three OP assays to the PM field samples extracted by rotating agitation.

2.4 Spatial Mapping

Spatial mapping of OP^{AA}, OP^{DCFH} and OP^{DTT} was performed by the software ArcMap 10.3.1 (ArcGis Desktop; ESRI, Redlands, CA, USA). The OP^{AA}, OP^{DCFH} and OP^{DTT} values obtained at the 23 sampling sites for each monitoring period were interpolated by using the spherical semivariogram model (Jian et al., 1996) of the ordinary kriging (OK) method (Johnston et al., 2001), in order to create a continuous surface from the 23 measured sample points and to predict the values at unmeasured locations (Kumar et al., 2007). OK is one of the most used kriging techniques for describing data spatial continuity (Gia Pham et al., 2019). The used OK estimator is given by a

linear combination of the observed values with weights, which are derived from the kriging equations, using experimental semivariances fitted by a spherical function (Xie et al., 2011).

3. Results and Discussion

3.1 PM_{10} Mass Concentration

Spatially-resolved data obtained by sampling in parallel at the 23 sites during the three monitoring periods allowed us to evaluate the spatial variability of PM_{10} mass concentration in Terni. PM_{10} mass concentrations determined in February, April and December 2017 are reported in Table 1.

From Table 1, we can observe that the concentration increased at all the sampling sites in the winter monitoring periods (February and December). Mean PM_{10} mass concentration was: 41 ± 7 μg m^{-3} in February, 19 ± 5 μg m^{-3} in April and 33 ± 7 μg m^{-3} in December. This behavior is mostly due to frequent temperature inversions during the colder season, which lead to severe episodes of atmospheric stability (Moroni et al., 2013; Curci et al., 2015), and to the major strength of typical winter sources, such as domestic biomass heating. In fact, in both February and December, high PM_{10} mass concentration was recorded at sites located near townhouses heated by biomass burning appliances (FR, BR and AR).

Table 1. PM_{10} mass concentration determined at the 23 sampling sites in the three monitoring periods (February, April and December 2017).

Site	PM_{10} Mass Concentration (μg m^{-3})		
	February	**April**	**December**
RI	52	21	44
MA	38	22	32
FA	33	21	38
GI	39	15	23
FR	46	12	32
CB	31	23	24
PI	40	18	34
BR	51	24	48
AR	34	14	36
CR	38	21	32
HG	53	10	35
SA	29	15	22
PV	47	21	34
LG	47	28	36
CZ	48	15	39
HV	45	16	35
UC	33	20	24
CA	46	20	36
CO	44	20	35
RO	40	16	29
OB	41	21	30

PR	32	30	26
CP	32	20	24
Mean	**41**	**19**	**33**
SD	**7**	**5**	**7**

227 *3.2 Spatial Mapping of OP*

228 Spatial variability of OP^{AA}, OP^{DCFH} and OP^{DTT} was evaluated, the OP values obtained at the 23
229 sites in the three monitoring periods are reported in supplementary material S2. Spatial mapping of
230 OP^{AA}, OP^{DCFH} and OP^{DTT} allowed us to assess spatial relationships between the three OP assays
231 and local emission sources of PM.

232 From Fig. 3, we can observe that high OP^{AA} values were recorded at sites close to the railway. In
233 particular, the highest OP^{AA} values were found at the sites located near the rail station (GI, CR and
234 HG), where trains brake entering the residential area of the city, releasing the highest amount of
235 dust by abrasion of rolling stock (Massimi et al., 2020b). Therefore, AA assay seems to be
236 particularly sensitive toward particles released from the rail network by mechanical abrasion of
237 train brakes. This source releases particles rich in some transition metals, such as Cu, Fe and Mn
238 (Abbasi et al., 2012; Querol et al., 2012; Kam et al., 2013; Namgung et al., 2016). In various
239 studies, OP^{AA} was found to be sensitive to transition metals (Vidrio et al., 2008; Charrier and
240 Anastasio, 2011; Simonetti et al., 2018b; Piacentini et al., 2019) and has been strongly positively
241 correlated with the main elements tracing non-exhaust traffic emission, such as Cu, Fe and Mn
242 (Shiraiwa et al., 2017; Pietrogrande et al., 2018a, 2018b; Bates et al., 2019). However, these
243 elements, generally considered as robust tracers of vehicular traffic, in Terni were found to be
244 released at much higher concentration from the railway (Massimi et al., 2020b). Moreover, these
245 results confirmed the high OP^{AA} activity shown at underground station in Gupta et al. (2019). It is
246 worth nothing that relative high OP^{AA} values were recorded at the sites influenced by the rail
247 network emission in all the monitoring periods, in accordance with the non-seasonal character of
248 this source. In April (panel b), the OP^{AA} response to particles released from the railway, turned out
249 to be higher and more localized at GI, CR and HG, presumably because of the more efficient
250 mixing of the lower atmosphere during the warmer season, which led to a less horizontal diffusion
251 of the released particles.

252 On the other hand, in Fig. 4 we can note that high OP^{DCFH} values were recorded at sites close to the
253 steel plant (RO, OB, PR and CO) in all the monitoring periods and at sites near townhouses
254 frequently heated by biomass burning appliances (BR, AR and CR) in winter (panels a and c). In
255 this case, the high OP^{DCFH} values recorded at BR, AR and CR in February (panel a) and December
256 (panel c), confirmed the relationships between OP^{DCFH} and PM released by domestic biomass
257 heating. In fact, in previous studies, the same sites were identified as the most impacted by biomass

burning contributions (Massimi et al., 2020a; 2020b). Relative high OP^{DCFH} values were also recorded at RO, OB, PR and CO in all the monitoring periods. These sites are close to the steel plant and have proven to be the most affected by particles released from the steel plant by abrasive machining of steel from the rolling plants and/or by combustive processes from the furnaces for the annealing of the cold rolled product (Massimi et al., 2020b). The relevance of steel plant related emissions on OP^{DCFH} values is particularly evident in April (panel b), when the strength of biomass burning emissions is weaker. Hence, DCFH assay seems to be particularly sensitive toward particles released from the steel plant and partly from domestic biomass heating. It is worth mentioning that in February, increased OP^{DCFH} values were also measured at sites near the railway (GI, CR and HG); this indicates a contribution to OP^{DCFH} also from particles released by abrasion of rolling stock. These results are in agreement with the findings of See et al. (2007) and Wang et al. (2010), which have shown a positive correlation between ROS and both transition metals (including Fe) and organic concentrations.

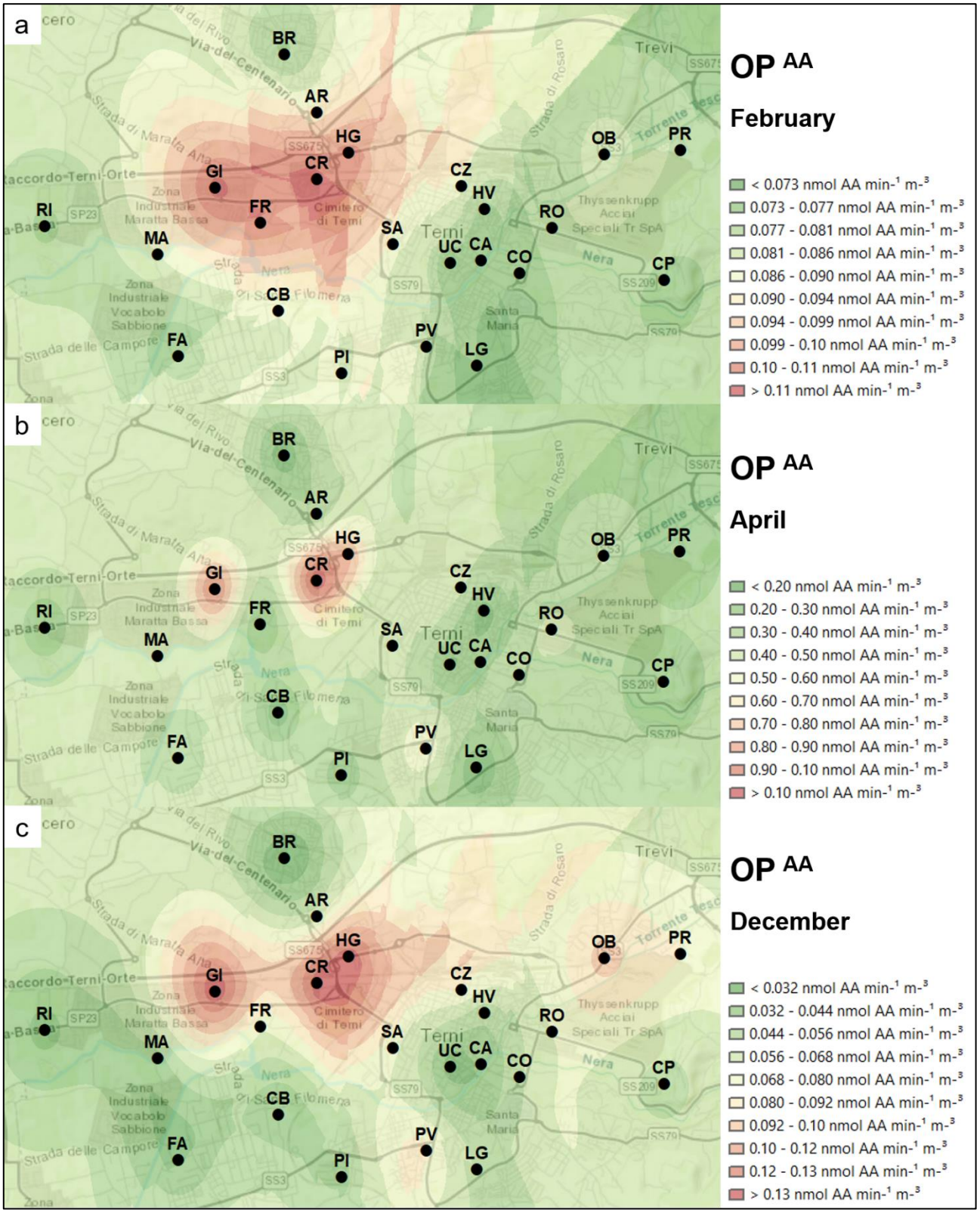

Fig. 3. Spatial mapping of OP^{AA} in February (panela a), April (panel b) and December (panel c) 2017.

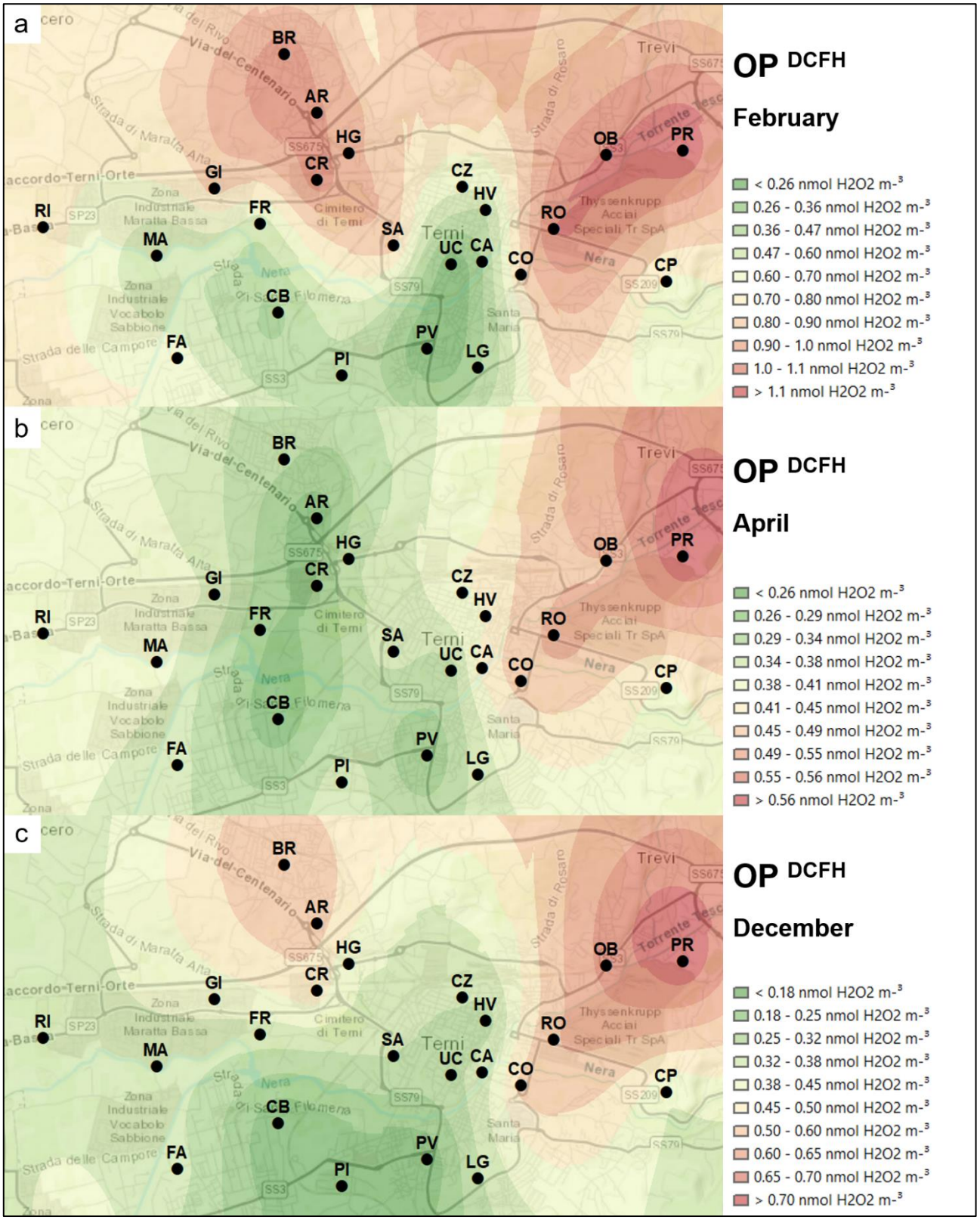

Fig. 4. Spatial mapping of OP^{DCFH} in February (panela a), April (panel b) and December (panel c) 2017.

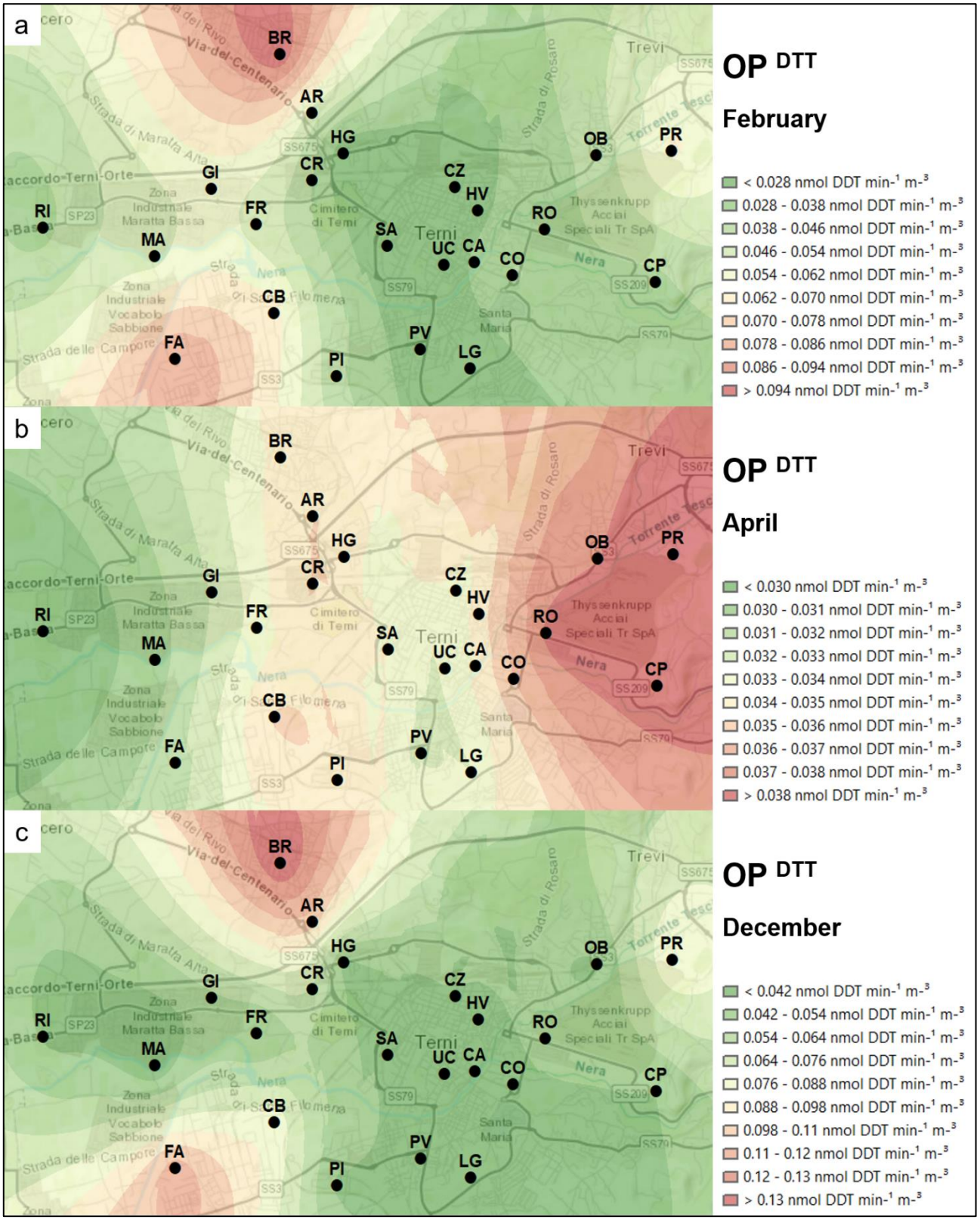

Fig. 5. Spatial mapping of OP^{DTT} in February (panela a), April (panel b) and December (panel c) 2017.

Finally, from Fig. 5, we can observe that in February (panel a) and December (panel c), the highest OP^{DTT} values were recorded at sites close to townhouses where domestic biomass heating systems

are prevalent (BR and AR) and at FA and CB. Previous studies demonstrated that these sites were affected by the emissions from burning of carpentry waste products (Massimi et al., 2020a; 2020b). Moreover, relative high OP^{DTT} values (supplementary material S2) occurred in all the monitoring periods at PR, which is the site most impacted by a source related to combustive processes associated to the steel production, such as casting, annealing and hot rolling of steel. This source releases particles rich of water-soluble Cr, Ga, Li, Mn and Zn (Massimi et al., 2020b). In April (panel b), when biomass burning appliances are not used, OP^{DTT} values turned out to be lower in all the Terni basin, except for the area affected by the steel plant (RO, OB, PR, CO and CP), where the highest OP^{DTT} values were recorded. Therefore, in general, DTT assay appears to be ~~specifically~~ sensitive to combustion sources, in particular, toward particles released by both industrial (panel b) and biomass burning (panel a and c) emissions. However, since biomass burning has a seasonal trend, a strong variability of the OP^{DTT} values at the sites influenced by this source is observed in the three monitoring periods, due to the stronger biomass burning contribution in the colder season. In fact, biomass burning and secondary organic aerosols are deemed to be the largest contributors to the OP^{DTT} (Verma et al., 2018). To corroborate this, despite various chemical components in atmospheric aerosols have been demonstrated to be well-correlated with OP^{DTT}, including water-soluble transition metal ions, water-soluble organic compounds and quinones (Wong et al., 2019), numerous studies have shown strong correlations of OP^{DTT} with K, a robust biomass burning tracer, and organic compounds, such as levoglucosan, associated to wood combustion sources (Pietrogrande et al., 2018a; Bates et al., 2019; Wang et al., 2019; Hakimzadeh et al., 2020).

3.3 Size *Distribution of OP*

Size distribution of OP^{AA}, OP^{DCFH} and OP^{DTT} was evaluated by analyzing size-segregated PM samples collected at CA, MA and PR. The OP^{AA}, OP^{DCFH} and OP^{DTT} values recorded in each size fraction at CA, MA and PR are reported in supplementary material S3.

Fig. 6 shows the mean concentration of the PM mass and the mean size distribution of the OP in Terni. Size distribution of PM mass concentration showed a bimodal profile, while OP^{AA}, OP^{DCFH} and OP^{DTT} size profiles were substantially unimodal, since AA, DCFH and DTT assays responded selectively to fine or coarse particles. In fact, from Fig. 6, we can observe that AA assay was found to be mainly sensitive to coarse particles (1.8-10 μm), showing a broad maximum in the size range 3.2-5.6 μm, while DCFH and DTT assays turned out to be more sensitive toward the fine fraction of PM (0.18-1.8 μm), with the highest OP values in the size fractions 0.56-1 μm and 0.32-0.56 μm, respectively. These findings are in line with previous publications, which have demonstrated higher OP^{AA} sensitivity toward redox active components in coarse aerosols (Godri et al., 2011; Manigrasso

et al., 2020) and higher OP^{DCFH} and OP^{DTT} values in the fine fraction of PM (De Vizcaya-Ruiz et al., 2006; Ntziachristos et al., 2007; Steenhof et al., 2011; Janssen et al., 2014). Moreover, these results confirmed the findings of paragraph 3.2. In fact, particles released by re-suspension of dust and mechanical processes, such as brake abrasion, to whom OP^{AA} was found to be more sensitive, are typically present in the coarse fraction of PM. On the contrary, combustion processes (such as biomass burning and hot works from the furnaces of the steel plant), to whom OP^{DCFH} and OP^{DTT} appeared to be more sensitive, mainly produce particles belonging to the fine fraction of PM (Shiraiwa et al., 2017; Canepari et al., 2019), which contain water-soluble metals and organics, generally associated with higher intrinsic redox activity.

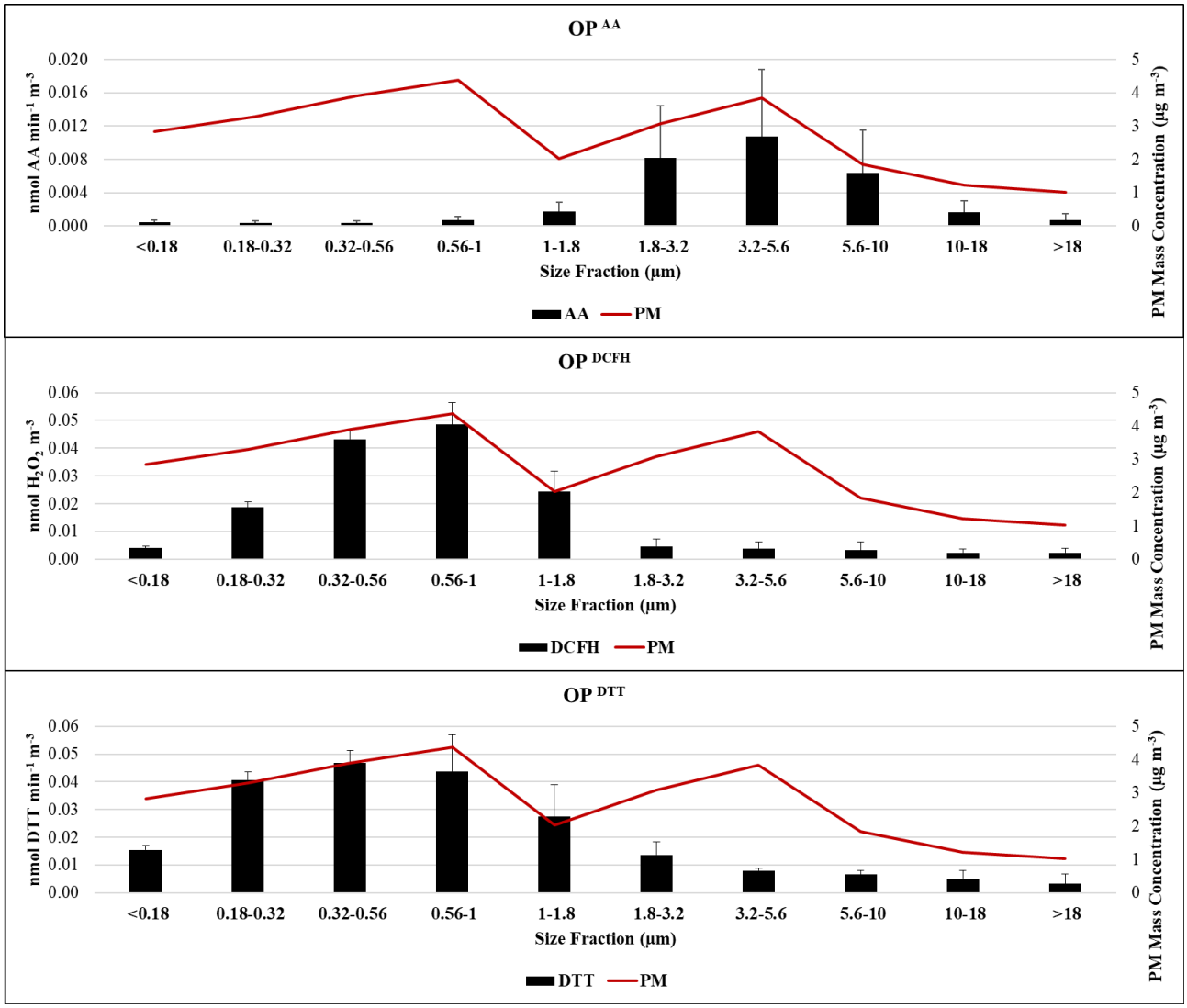

Fig. 6. Mean concentration of the PM mass and mean OP^{AA}, OP^{DCFH} and OP^{DTT} values of size-segregated PM samples collected at CA, MA and PR.

4. Conclusions

In this study, an innovative experimental approach, based on the spatial mapping of OP^{AA}, OP^{DCFH} and OP^{DTT}, for geo-referenced assessment of PM potential to induce oxidative stress, was described. This approach allowed us to map the spatial variability of OP^{AA}, OP^{DCFH} and OP^{DTT}, proving to be a powerful tool, transferable to other monitoring campaigns, for the individuation of spatial relationships between oxidative potential of PM and its chemical composition and sources. The obtained results showed that OP^{AA} was particularly sensitive toward coarse particles (1.8-10 μm) released from the rail network (GI, CR and HG) by abrasion of train brakes. On the contrary, OP^{DCFH} appeared to be particularly sensitive to fine particles (0.18-1.8 μm) released from the steel plant (RO, OB, PR and CO) and domestic biomass heating (BR, AR and CR), while OP^{DTT} was found to be specifically sensitive toward the fine fraction of PM (0.18-1.8 μm) released by both industrial and biomass burning sources, such as domestic biomass heating (BR and AR) and the burning of carpentry waste products (FA and CB). Overall, these results showed that biomass burning may play a key role in PM potential to generate ROS.

The described approach promises to be very effective for the identification and localization of the emission sources mainly responsible for ROS generation and provides a reliable tool for spatially-resolved evaluation of exposure to PM and relative health risk.

Acknowledgments

This work was funded by the project 2017 RG11715C7C8801CF (Principal Investigator Dr. S. Canepari) and the project 2019 AR11916B7027C1E6 (Principal Investigator Dr. L. Massimi), financed by Sapienza University of Rome.

The authors gratefully thank FAI Instruments (Fonte Nuova, Rome, Italy), the citizens of Terni and the Terni district of ARPA Umbria (regional agency for environmental protection), with special regard to Giancarlo Caiello, Caterina Austeri and Marco Pompei, for the support in the installation and management of the sampling equipment as well as for the help in the choice of the sampling sites. Moreover, the authors warmly thank C.N.R. Institute of Atmospheric Pollution Research, with special regard to Cinzia Perrino, for having made available the low-pressure cascade impactors used in this study.

Author Contributions: L. Massimi and S. Canepari conceived and planned the monitoring and the experiments; L. Massimi and M. Ristorini performed the samplings; L. Massimi, M. Ristorini and G. Simonetti performed the OP analyses; L. Massimi and G. Simonetti elaborated the data; L. Massimi wrote the manuscript; M. A. Frezzini and M. L. Astolfi reviewed a previous version of the manuscript; L. Massimi and S. Canepari coordinated the group and supervised the manuscript.

Conflicts of Interest: The authors declare no conflicts of interest.

References

Abbasi, S., Olander, L., Larsson, C., Olofsson, U., Jansson, A., Sellgren, U. 2012. A field test study of airborne wear particles from a running regional train. Proceedings of the Institution of Mechanical Engineers, Part F: Journal of Rail and Rapid Transit, 226(1), 95-109.

Anderson, J. O., Thundiyil, J. G., Stolbach, A. 2012. Clearing the air: a review of the effects of particulate matter air pollution on human health. Journal of Medical Toxicology, 8(2), 166-175.

Ayres, J. G., Borm, P., Cassee, F. R., Castranova, V., Donaldson, K., Ghio, A., Harrison, R.M., Hider, R., Kelly, F., Kooter, I.M., Marano, F., Maynard, R.L., Mudway, I., Nel, A., Sioutas, C., Smith, S., Baeza-Squiban, A., Cho, A., Duggan, S., Froines, J. 2008. Evaluating the toxicity of airborne particulate matter and nanoparticles by measuring oxidative stress potential - a workshop report and consensus statement. Inhalation Toxicology, 20(1), 75-99.

Bates, J. T., Fang, T., Verma, V., Zeng, L., Weber, R. J., Tolbert, P. E., Abrams, J. Y., Sarnat, S. E., Klein, M., Mulholland, J. A., Russell, A. G. 2019. Review of acellular assays of ambient particulate matter oxidative potential: Methods and relationships with composition, sources, and health effects. Environmental Science & Technology, 53(8), 4003-4019.

Brunekreef, B., Holgate, S. T. 2002. Air Pollution and Health. Lancet 360, 1233–1242.

Calas, A., Uzu, G., Kelly, F., Houdier, S., Martins, J., Thomas, F., Molton, F., Charron, A., Dunster, C., Oliete, A., Jacob, V., Besombes, J., Chevrier, F., Jaffrezo, J. 2018. Comparison between five acellular oxidative potential measurement assays performed with detailed chemistry on PM10 samples from the city of Chamonix (France). Atmospheric Chemistry and Physics, 18, 7863–7875.

Campbell, S. J., Utinger, B., Lienhard, D. M., Paulson, S. E., Shen, J., Griffiths, P. T., Stell, A.C., Kalberer, M. 2019. Development of a physiologically relevant online chemical assay to quantify aerosol oxidative potential. Analytical Chemistry, 91(20), 13088-13095.

Canepari, S., Astolfi, M. L., Catrambone, M., Frasca, D., Marcoccia, M., Marcovecchio, F., Massimi, L., Rantica, E., Perrino, C. 2019. A combined chemical/size fractionation approach to

study winter/summer variations, ageing and source strength of atmospheric particles. Environmental Pollution, 253, 19-28.

Capelli, L., Sironi, S., Del Rosso, R., Céntola, P., Rossi, A., Austeri, C. 2011. Olfactometric approach for the evaluation of citizens' exposure to industrial emissions in the city of Terni, Italy. Science of the Total Environment, 409(3), 595-603.

Catrambone, M., Canepari, S., Cerasa, M., Sargolini, T., Perrino, C. 2019. Performance evaluation of a very-low-volume sampler for atmospheric particulate matter. Aerosol Air Quality Research, 19, 2160-2172.

Cesari, D., Merico, E., Grasso, F. M., Decesari, S., Belosi, F., Manarini, F., De Nuntiis, P., Rinaldi, M., Volpi, F., Gambaro, A., Morabito, E., Contini, D. 2019. Source apportionment of PM2.5 and of its oxidative potential in an industrial suburban site in south Italy. Atmosphere, 10(12), 758.

Charrier, J. G., Anastasio, C. 2011. Impacts of antioxidants on hydroxyl radical production from individual and mixed transition metals in a surrogate lung fluid. Atmospheric Environment, 45 (40), 7555− 7562.

Chirizzi, D., Cesari, D., Guascito, M. R., Dinoi, A., Giotta, L., Donateo, A., Contini, D. 2017. Influence of Saharan dust outbreaks and carbon content on oxidative potential of water-soluble fractions of PM2.5 and PM10. Atmospheric Environment, 163, 1–8.

Cho, A. K., Sioutas, C., Miguel, A. H., Kumagai, Y., Schmitz, D. A., Singh, M., Fernandez, F.A., Froines, J. R. 2005. Redox activity of airborne particulate matter at different sites in the Los Angeles Basin. Environmental Research, 99(1), 40-47.

Curci, G., Ferrero, L., Tuccella, P., Barnaba, F., Angelini, F., Bolzacchini, E., Carbone, C., Denier van der Gon, H. A. C., Facchini, M. C., Gobbi, G. P., Kuenen, J. P. P., Landi, T. C., Perrino, C., Perrone, M. G., Sangiorgi, G., Stocchi, P. 2015. How much is particulate matter near the ground influenced by upper-level processes within and above the PBL? A summertime case study in Milan (Italy) evidences the distinctive role of nitrate. Atmospheric Chemistry and Physics, 15(5), 2629-2649.

Delfino, R. J., Staimer, N., Vaziri, N. D. 2011. Air pollution and circulating biomarkers of oxidative stress. Air Quality, Atmosphere & Health, 4(1), 37-52.

De Vizcaya-Ruiz, A., Gutiérrez-Castillo, M. E., Uribe-Ramirez, M., Cebrián, M. E., Mugica-Alvarez, V., Sepúlveda, J., Rosas, I., Salinas, E., Garcia-Cue´llar, C., Martinez, F., Alfaro-Moreno, E., Torres-Flores, V., Osornio-Vargas, A., Sioutas, C., Fine, P.M., Singh, M., Geller, M.D., Kuhn, T., Miguel, A.H., Eiguren-Fernandez, A., Schiesti, R.H., Reliene, R., Froines, J. 2006. Characterization and in vitro biological effects of concentrated particulate matter from Mexico City. Atmospheric Environment, 40, 583-592.

Fang, T., Verma, V., Bates, J. T., Abrams, J., Klein, M., Strickland, M. J., Sarnat, S. E., Chang, H. H., Mulholland, J. A., Tolbert, P. E., Russell, A. G. 2015. Oxidative potential of ambient water-soluble PM 2.5 measured by Dithiothreitol (DTT) and Ascorbic Acid (AA) assays in the southeastern United States: contrasts in sources and health associations. Atmospheric Chemistry & Physics Discussions, 15(21) 30609-30644.

Fang, T., Verma, V., Bates, J. T., Abrams, J., Klein, M., Strickland, M. J., Stefanie E., Sarnat, S. E., Chang, H. H., Mulholland, J. A., Tolbert, P. E., Russell, A. G., Weber, R. J. 2016. Oxidative Potential of Ambient Water-Soluble PM2.5 in the Southeastern United States: Contrasts in Sources and Health Associations between Ascorbic Acid (AA) and Dithiothreitol (DTT) Assays. Atmospheric Chemistry, 16, 3865–3879.

Ferrero, L., Cappelletti, D., Moroni, B., Sangiorgi, G., Perrone, M. G., Crocchianti, S., Bolzacchini, E. 2012. Wintertime aerosol dynamics and chemical composition across the mixing layer over basin valleys. Atmospheric Environment, 56, 143-153.

Frezzini, M. A., Castellani, F., De Francesco, N., Ristorini, M., Canepari, S. 2019. Application of DPPH Assay for Assessment of Particulate Matter Reducing Properties. Atmosphere, 10(12), 816.

Gao, D., Mulholland, J. A., Russell, A. G., Weber, R. J. 2020. Characterization of water-insoluble oxidative potential of PM2.5 using the dithiothreitol assay. Atmospheric Environment, 224, 117327.

Gia Pham, T., Kappas, M., Van Huynh, C., Hoang Khanh Nguyen, L. 2019. Application of ordinary kriging and regression kriging method for soil properties mapping in hilly region of Central Vietnam. ISPRS International Journal of Geo-Information, 8(3), 147.

Giorio, C., Tapparo, A., Scapellato, M.L., Carrieri, M., Apostoli, P., Bartolucci, G.B. 2013. Field comparison of a personal cascade impactor sampler, an optical particle counter and CEN-EU

443 standard methods for PM10, PM2.5 and PM1 measurement in urban environment. Journal of
444 Aerosol Science, 65, 111-120.

445 Godri, K. J., Harrison, R. M., Evans, T., Baker, T., Dunster, C., Mudway, I. S., Kelly, F. J. 2011.
446 Increased oxidative burden associated with traffic component of ambient particulate matter at
447 roadside and urban background schools sites in London. PloS one, 6(7).

448 Guerrini, R. 2012. Qualità dell'aria nella provincia di Terni tra il 2002 e il 2011. Quad ARPA
449 Umbria, 81-87.

450 Gupta, T., Singh, S. P., Rajput, P., Agarwal, A. K. 2019. Measurement, Analysis and Remediation
451 of Environmental Pollutants. Springer.

452 Hakimzadeh, M., Soleimanian, E., Mousavi, A., Borgini, A., De Marco, C., Ruprecht, A. A.,
453 Sioutas, C. 2020. The impact of biomass burning on the oxidative potential of PM2. 5 in the
454 metropolitan area of Milan. Atmospheric Environment, 224, 117328.

455 Halliwell, B., Whiteman, M. 2004. Measuring reactive species and oxidative damage *in vivo* and in
456 cell culture: How should you do it and what do the results mean? British Journal of Pharmacology,
457 142, 231–255.

458 Hlavay, J., Polyak, K., Weisz, M. 2001. Monitoring of the natural environment by chemical
459 speciation of elements in aerosol and sediment samples. Presented at the Whistler 2000 Speciation
460 Symposium, Whistler Resort, BC, Canada, June 25–July 1, 2000. Journal of Environmental
461 Monitoring, 3(1), 74-80.

462 Huang, W., Zhang, Y., Zhang, Y., Fang, D., Schauer, J. J., 2016. Optimization of the Measurement
463 of Particle-Bound Reactive Oxygen Species with 2',7'-dichlorofluorescin (DCFH), Water Air Soil
464 Pollution, 227, 164.

465 Hung, H. F., Wang, C. S. 2001. Experimental determination of reactive oxygen species in Taipei
466 aerosols. Journal of Aerosol Science, 32, 1201–1211.

467 Janssen, N. A., Yang, A., Strak, M., Steenhof, M., Hellack, B., Gerlofs-Nijland, M. E., Kuhlbusch
468 T., Kelly, F., Harrison R., Brunekreef, B., Cassee, F., Hoek, G. 2014. Oxidative potential of
469 particulate matter collected at sites with different source characteristics. Science of the Total
470 Environment, 472, 572-581.

471 Jian, X., Olea, R. A., Yu, Y. S. 1996. Semivariogram modeling by weighted least squares.
472 Computers & Geosciences, 22(4), 387-397.

473 Johnston, K., Ver Hoef, J. M., Krivoruchko, K., Lucas, N. 2001. Using ArcGIS geostatistical
474 analyst (Vol. 380). Redlands: Esri.

475 Kam, W., Delfino, R. J., Schauer, J. J., Sioutas, C. 2013. A comparative assessment of PM2.5
476 exposures in light-rail, subway, freeway, and surface street environments in Los Angeles and
477 estimated lung cancer risk. Environmental Science: Processes & Impacts, 15(1), 234-243.

478 Kelly, F. J., Fuller, G. W., Walton, H. A., Fussell, J. C. 2012. Monitoring air pollution: Use of early
479 warning systems for public health. Respirology, 17(1), 7-19.

480 Khurshid, S. S., Siegel, J. A., Kinney, K. A. 2014. Indoor particulate reactive oxygen species
481 concentrations. Environmental research, 132, 46-53.

482 Kumar, A., Maroju, S., Bhat, A. 2007. Application of ArcGIS geostatistical analyst for interpolating
483 environmental data from observations. Environmental Progress, 26(3), 220-225.

484 Lebel, C. P., Ischiropoulos, H., Bondy, S. C. 1992. Evaluation of the probe 2',7'-dichlorofluorescin
485 as an indicator of reactive oxygen species formation and oxidative stress. Chemical Research in
486 Toxicology, 5, 227–231.

487 Li, R., Kou, X., Geng, H., Xie, J., Yang, Z., Zhang, Y., Cai, Z., Dong, C. 2015. Effect of ambient
488 PM 2.5 on lung mitochondrial damage and fusion/fission gene expression in rats. Chemical
489 Research in Toxicology, 28, 408-418.

490 Lubczyńska, M. J., Sunyer, J., Tiemeier, H., Porta, D., Kasper-Sonnenberg, M., Jaddoe, V. W.,
491 Xavier Basagaña, X., Dalmau-Bueno, A., Forastiere, F., Wittsiepe, J., Hoffmann, B.,
492 Nieuwenhuijsen, M., Hoek, G., de Hoogh, K., Brunekreef, B., Guxens, M. 2017. Exposure to
493 elemental composition of outdoor PM2.5 at birth and cognitive and psychomotor function in
494 childhood in four European birth cohorts. Environment international, 109, 170-180.

495 Manigrasso, M., Simonetti, G., Astolfi, M. L., Perrino, C., Canepari, S., Protano, C., Antonucci, A.,
496 Avino, P., Vitali, M. 2020. Oxidative Potential Associated with Urban Aerosol Deposited into the
497 Respiratory System and Relevant Elemental and Ionic Fraction Contributions. Atmosphere, 11(1),
498 6.

Marcoccia, M., Ronci, L., De Matthaeis, E., Setini, A., Perrino, C., Canepari, S. 2017. In-vivo assesment of the genotoxic and oxidative stress effects of particulate matter on *Echinogammarus veneris*. Chemosphere, 173, 124–134.

Massimi, L., Ristorini, M., Eusebio, M., Florendo, D., Adeyemo, A., Brugnoli, D., Canepari, S. 2017. Monitoring and evaluation of Terni (Central Italy) air quality through spatially resolved analyses. Atmosphere, 8(10), 200.

Massimi, L., Conti, M. E., Mele, G., Ristorini, M., Astolfi, M. L., Canepari, S. 2019. Lichen transplants as indicators of atmospheric element concentrations: a high spatial resolution comparison with PM_{10} samples in a polluted area (Central Italy). Ecological Indicators, 101, 759-769.

Massimi, L., Simonetti, G., Buiarelli, F., Di Filippo, P., Pomata, D., Riccardi, C., Ristorini, M., Astolfi, M.L., Canepari, S. 2020a. Spatial distribution of levoglucosan and alternative biomass burning tracers in atmospheric aerosols, in an urban and industrial hot-spot of Central Italy. Atmospheric Research, 104904.

Massimi, L., Ristorini, M., Astolfi, M.L., Perrino, C., Canepari, S. 2020b. High Resolution Spatial Mapping of Element Concentrations in PM_{10}: a Powerful Tool for Localization of Emission Sources. Atmospheric Research, 105060.

Miljevic, B., Hedayat, F., Stevanovic, S., Fairfull-Smith, K. E., Bottle, S. E., Ristovski, Z. D. 2014. To sonicate or not to sonicate PM filters: Reactive oxygen species generation upon ultrasonic irradiation. Aerosol science and technology, 48(12), 1276-1284.

Morini, E., Touchaei, A. G., Castellani, B., Rossi, F., Cotana, F. 2016. The impact of albedo increase to mitigate the urban heat island in Terni (Italy) using the WRF model. Sustainability, 8(10), 999.

Mutzel, A., Rodigast, M., Iinuma, Y., Böge, O., Herrmann, H. 2013. An improved method for the quantification of SOA bound peroxides. Atmospheric Environment, 67, 365-369.

Namgung, H. G., Kim, J. B., Woo, S. H., Park, S., Kim, M., Kim, M. S., Bae, G. N., Park, D., Kwon, S. B. 2016. Generation of nanoparticles from friction between railway brake disks and pads. Environmental Science and Technology, 50(7), 3453-3461.

Ntziachristos, L., Froines, J. R., Cho, A. K., Sioutas, C. 2007. Relationship between redox activity and chemical speciation of size-fractionated particulate matter. Particle and Fibre Toxicology, 4(1), 5.

Øvrevik, J. 2019. Oxidative potential versus biological effects: A review on the relevance of cell-free/abiotic assays as predictors of toxicity from airborne particulate matter. International Journal of Molecular Sciences, 20, 4772.

Perrone, M. G., Zhou, J., Malandrino, M., Sangiorgi, G., Rizzi, C., Ferrero, L., Dommen, J., Bolzacchini, E. 2016. PM chemical composition and oxidative potential of the soluble fraction of particles at two sites in the urban area of Milan, Northern Italy. Atmospheric Environment, 128, 104-113.

Pietrogrande, M. C., Perrone, M. R., Manarini, F., Romano, S., Udisti, R., Becagli, S. 2018a. PM10 oxidative potential at a Central Mediterranean Site: Association with chemical composition and meteorological parameters. Atmospheric Environment, 188, 97-111.

Pietrogrande, M. C., Dalpiaz, C., Dell'Anna, R., Lazzeri, P., Manarini, F., Visentin, M., Tonidandel, G. 2018b. Chemical composition and oxidative potential of atmospheric coarse particles at an industrial and urban background site in the alpine region of northern Italy. Atmospheric Environment, 191, 340-350.

Piacentini, A., Falasca, G., Canepari, S., Massimi, L. 2019. Potential of PM-selected components to induce oxidative stress and root system alteration in a plant model organism. Environment International, 132, 105094.

Pope III, C. A., Dockery, D. W. 2006. Health effects of fine particulate air pollution: Lines that connect. Journal of the Air & Waste Management Association, 56, 709–742.

Querol, X., Moreno, T., Karanasiou, A., Reche, C., Alastuey, A., Viana, M., Font, O., Gil, J., de Miguel, E., Capdevila, M. 2012. Variability of levels and composition of PM10 and PM2.5 in the Barcelona metro system. Atmospheric Chemistry and Physics, 12(11), 5055-5076.

Ricci, P. F., Cirillo, M. C. 1985. Uncertainty in health risk analysis. Journal of Hazardous Materials, 10(2-3), 433-447.

Ristorini, M., Astolfi, M.L., Frezzini, M.A., Canepari, S., Massimi, L. 2020. Evaluation of the efficiency of Arundo donax L. leaves as biomonitors for atmospheric element concentrations in an urban and industrial area of Central Italy. Atmosphere, 11(3), 226.

557 See, S. W., Wang, Y. H., Balasubramanian, R. 2007. Contrasting reactive oxygen species and
558 transition metal concentrations in combustion aerosols. Environmental Research, 103(3), 317-324.

559 SENTIERI-ReNaM, GdL, Binazzi, A., Mangone, L. 2016. SENTIERI - Epidemiological study of
560 residents in national priority contaminated sites: incidence of mesothelioma. Epidemiologia e
561 Prevenzione, 40 (5 Suppl1), 1-116.

562 Sgrigna, G., Sæbø, A., Gawronski, S., Popek, R., Calfapietra, C. 2015. Particulate Matter deposition
563 on Quercus ilex leaves in an industrial city of central Italy. Environmental Pollution, 197, 187-194.

564 Shiraiwa, M., Ueda, K., Pozzer, A., Lammel, G., Kampf, C. J., Fushimi, A., Enami, S., Arangio,
565 A.M., Fröhlich-Nowoisky, J., Fujitani,, Y., Furuyama, A., Lakey, P.S.J., Lelieveld, J., Lucas, K.,
566 Morino, Y., Pöschl, U., Takahama, S., Takami, A., Tong, H., Weber, B., Yoshino, A., Sato, K.
567 2017. Aerosol health effects from molecular to global scales. Environmental Science &
568 Technology, 51(23), 13545-13567.

569 Simonetti, G., Conte, E., Perrino, C., Canepari, S. 2018a. Oxidative potential of size-segregated PM
570 in a urban and an industrial area of Italy. Atmospheric Environment, 187, 292–300.

571 Simonetti, G., Conte, E., Massimi, L., Frasca, D., Perrino, C., Canepari, S. 2018b. Oxidative
572 potential of particulate matter components generated by specific emission sources. Journal of
573 Aerosol Sciences, 126, 99-109.

574 Steenhof, M., Gosens, I., Strak, M., Godri, K. J., Hoek, G., Cassee, F. R., Mudway, I.S., Kelly, F.J.,
575 Harrison, R.M., Lebret, E., Brunekreef, B., Janssen, N.A., Pieters, R.H. 2011. In vitro toxicity of
576 particulate matter (PM) collected at different sites in the Netherlands is associated with PM
577 composition, size fraction and oxidative potential-the RAPTES project. Particle and fibre
578 toxicology, 8(1), 26.

579 Stoeger, T., Takenaka, S., Frankenberger, B., Ritter, B., Karg, E., Maier, K., Shulz, H., Schmid, O.
580 2009. Deducing in vivo toxicity of combustion-derived nanoparticles from a cell-free oxidative
581 potency assay and metabolic activation of organic compounds. Environmental Health
582 Perspectives, 117(1), 54-60.

583 Strak, M., Janssen, N. A., Godri, K. J., Gosens, I., Mudway, I. S., Cassee, F. R., Lebret, E., Kelly,
584 F.G., Harrison, M.R., Brunekreef, B., Steenhof, M., Hoek, G. 2012. Respiratory health effects of
585 airborne particulate matter: the role of particle size, composition, and oxidative potential - the
586 RAPTES project. Environmental Health Perspectives, 120(8), 1183-1189.

587 Venkatachari, P., Hopke, P. K., Grover, B. D., Eatough, D. J. 2005. Measurement of particle-bound
588 reactive oxygen species in rubidoux aerosols. Journal of Atmospheric Chemistry, 50, 49–58.

589 Venkatachari, P., Hopke, P. K., Brune, W. H., Ren, X., Lesher, R., Mao, J., Mitchell, M. 2007.
590 Characterization of wintertime reactive oxygen species concentrations in Flushing, New York.
591 Aerosol Science and Technology, 41, 97–111.

592 Verma, V., Sioutas, C., Weber, R. J. 2018. Oxidative Properties of Ambient Particulate Matter - An
593 Assessment of the Relative Contributions from Various Aerosol Components and Their Emission
594 Sources. Multiphase Environmental Chemistry in the Atmosphere, 389–416.

595 Vidrio, E., Jung, H., Anastasio, C. 2008. Generation of hydroxyl radicals from dissolved transition
596 metals in surrogate lung fluid solutions. Atmospheric Environment, 42 (18), 4369−4379.

597 Wang, H., Joseph, J. A. 1999. Quantifying cellular oxidative stress by dichlorofluorescein assay
598 using microplate reader. Free Radical Biology & Medicine, 27, 612–616.

599 Wang, Y., Arellanes, C., Curtis, D. B., Paulson, S. E. 2010. Probing the source of hydrogen
600 peroxide associated with coarse mode aerosol particles in Southern California. Environmental
601 Science & Technology, 44(11), 4070-4075.

602 Wang, M., Beelen, R., Eeftens, M., Meliefste, K., Hoek, G., Brunekreef, B. 2012. Systematic
603 evaluation of land use regression models for NO_2. Environmental Science & Technology, 46(8),
604 4481-4489.

605 Wang, J., Lin, X., Lu, L., Wu, Y., Zhang, H., Lv, Q., Liu, W., Zhang Y., Zhuang, S. 2019.
606 Temporal variation of oxidative potential of water soluble components of ambient PM2. 5 measured
607 by dithiothreitol (DTT) assay. Science of The Total Environment, 649, 969-978.

608 WHO 2013. Review of evidence on health aspects of air pollution – REVIHAAP. First Results.
609 WHO's Regional Office for Europe, Copenhagen, 28 pp., http://www.euro.who.int/ data/ assets/pdf
610 file/0020/182432/e96762-final.pdf, 2013.

611 Wong, J. P., Tsagkaraki, M., Tsiodra, I., Mihalopoulos, N., Violaki, K., Kanakidou, M., Sciare, J.,
612 Nenes, A., Weber, R. J. 2019. Effects of atmospheric processing on the oxidative potential of
613 biomass burning organic aerosols. Environmental Science & Technology, *53*(12), 6747-6756.

614 Xie, Y., Chen, T. B., Lei, M., Yang, J., Guo, Q. J., Song, B., Zhou, X. Y. 2011. Spatial distribution
615 of soil heavy metal pollution estimated by different interpolation methods: Accuracy and
616 uncertainty analysis. Chemosphere, 82(3), 468-476.

617 Yang, A., Janssen, N. A., Brunekreef, B., Cassee, F. R., Hoek, G., Gehring, U. 2016. Children's
618 respiratory health and oxidative potential of PM2.5: the PIAMA birth cohort study. Journal of
619 Occupational and Environmental Medicine, 73(3), 154-160.